hibit chemical and isotopic features that are similar to the shergottites. Although the major element chemistry will vary as a result of differentiation, minor and trace element ratios should have similar values, provided that the elements considered are not fractionated from each other during igneous processes. The surprisingly young (for a meteorite) radiometric age of crystallization determined for shergottites is $\sim 0.6 \times 10^9$ years (*10*), and a similar value may be obtained for ALHA 77005. If this new achondrite is older, it would suggest that ALHA 77005 represents a relict sample of the source peridotite from which the shergottites formed by later melting. Many of the remarkable similarities between terrestrial basaltic rocks and shergottites [chemistry, oxidation state, and potassium/uranium ratios (*4*)] should extend to ALHA 77005, as this new achondrite may provide an additional sample of the only other body in the solar system known to be similar in composition to the upper mantle of the earth.

HARRY Y. MCSWEEN, JR.
LAWRENCE A. TAYLOR
Department of Geological Sciences, University of Tennessee, Knoxville 37916

EDWARD M. STOLPER
Department of Geological Sciences, Harvard University, Cambridge, Massachusetts 02138

References and Notes

1. Meteorites which fall randomly over the continent are carried toward continental margins by moving ice. The Allan Hills provide a physical barrier for the ice so that meteorites are concentrated in a small area as ice is removed by ablation. Details of the Allan Hills site have been discussed by Y. Yanai, W. A. Cassidy, M. Funaki, and B. P. Glass [*Proc. 9th Lunar Planet. Sci. Conf.* (1978), p. 977].
2. Designations for Antarctic meteorites consist of an abbreviated location name (ALH), a letter designating the search party (A), and a five-digit number beginning with the December year of the austral summer season as the first two digits (77) followed by the meteorite sample number (005).
3. J. A. Wood, *Geotimes* **22**, 29 (1977); J. W. Head, C. A. Wood, T. A. Mutch, *Am. Sci.* **65**, 21 (1977).
4. E. M. Stolper and H. Y. McSween, Jr., *Geochim. Cosmochim. Acta*, in press; J. V. Smith and R. L. Hervig, *Meteoritics*, in press; M. B. Duke, in *Shock Metamorphism of Natural Materials* (Mono, Wilkes-Barre, Pa., 1968). p. 613.
5. B. Mason, *Antarct. Meteorite Newsl.* **1** (No. 2), 9 (1978).
6. T. E. Bunch and K. Keil, *Am. Mineral.* **56**, 146 (1971).
7. E. M. Stolper, H. Y. McSween, Jr., J. F. Hays, *Geochim. Cosmochim. Acta*, in press.
8. P. Stöffler, *Fortschr. Mineral.* **49**, 50 (1972).
9. J. L. Wooden, L. E. Nyquist, D. D. Bogard, B. M. Bansal, H. Wiesmann, C.-Y. Shih, G. A. McKay, *Lunar Planet. Sci.* **10**, 1379 (1979).
10. L. Nyquist, J. Wooden, B. Bansal, H. Wiesmann, G. McKay, D. Bogard, *Geochim. Cosmochim. Acta*, in press.
11. We thank the National Science Foundation and NASA for acquiring and making available these samples. This work was supported by NASA grant NSG-7413 to H.Y.M.

25 January 1979; revised 9 March 1979

Carbon Dioxide in the Ocean Surface: The Homogeneous Buffer Factor

Abstract. *The amount of carbon dioxide that can be dissolved in surface seawater depends at least partially on the homogeneous buffer factor, which is a mathematical function of the chemical equilibrium conditions among the various dissolved inorganic species. Because these equilibria are well known, the homogeneous buffer factor is well known. Natural spatial variations depend very systematically on sea surface temperatures, and do not contribute significantly to uncertainties in the present or future carbon dioxide budget.*

Injection of anthropogenic CO_2 into the atmosphere may cause a serious deterioration of global climate. It is likely that geochemical processes will eventually transfer much of this CO_2 to the oceans. The dissolution of atmospheric CO_2 in surface seawater is enhanced by the oceans' capacity to buffer the associated changes in seawater chemistry. The buffering capacity of seawater depends on the conditions and reactions that control the partitioning of carbon within the oceans. For example, reactions with carbonate minerals may tend to maintain relatively constant carbonate ion concentrations, or metabolic processes may buffer against changing pH conditions. We have chosen to examine the most frequently cited buffering mechanism: the homogeneous reaction of dissolved CO_2 with other dissolved inorganic species in seawater. Estimates of the effectiveness of this mechanism vary widely (*1*). Our calculations, using GEOSECS surface water data from the Atlantic and Pacific oceans, clarify some of these differences and their significance for global CO_2 models.

The homogeneous buffering mechanism is frequently evaluated in terms of the buffer factor (*2*)

$$\frac{dpCO_2/pCO_2}{dTCO_2/TCO_2}$$

where TCO_2 is the total concentration of dissolved inorganic carbon in surface seawater equilibrated with the atmospheric CO_2 partial pressure pCO_2. Because this homogeneous buffer factor excludes any heterogeneous reactions that might affect seawater total alkalinity (TA), it is more accurately defined as

$$B_{hom} = \left(\frac{\partial pCO_2}{\partial TCO_2}\right)_{TA} \times \frac{TCO_2}{pCO_2} \quad (1)$$

The homogeneous buffer factor refers by definition to an equilibrium state, and it can be calculated from the relevant equilibrium relationships. To "measure" B_{hom} in seawater is, in effect, to determine the appropriate equilibrium constants for a particular composition and temperature. Five sets of salinity- and temperature-dependent values for these constants have been published during the last 30 years (*3–8*). We have used them to calculate B_{hom} according to the equation

$$B_{hom} = TCO_2\left\{[H_2CO_3^*] + [CO_3^{2-}] + \frac{\gamma[HCO_3^-] - 4[CO_3^{2-}]^2}{[HCO_3^-] + 4[CO_3^{2-}] + \gamma}\right\}^{-1} \quad (2)$$

where

$$\gamma = \frac{TB(K_B')a_{H^+}}{(K_B' + a_{H^+})^2} \quad (3)$$

and a_{H^+} is the hydrogen ion activity , the brackets denote total single ion plus complex ion concentrations, $[H_2CO_3^*]$ is the sum of the concentrations of dissolved CO_2 and carbonic acid, TB is the total concentration of dissolved borate, and K_B' is the first apparent dissociation constant of boric acid (*9*).

Figure 1a shows that the different sets of constants yield B_{hom} values that agree within 0.5 percent in warm waters and 4 percent in cold waters. The constants of Buch (*3*) and Edmond and Gieskes (*5*) are not consistent with experiments performed as part of the GEOSECS program (*10*). If these two sets of constants are ignored, the maximum difference in Fig. 1a is less than 1 percent throughout the full range of sea surface temperatures.

Figure 1a also shows the maximum range of B_{hom} error that might be associated with published uncertainties in the GEOSECS TCO_2 and TA data (*10, 11*). These margins of error range from about $\pm$ 1 percent in warm waters to $\pm$ 3 percent in cold waters.

Figure 1b shows that natural spatial variations in the ocean mixed layer greatly exceed the analytical margins of error associated with B_{hom}. These spatial variations would seem to explain the broad range of published buffer factor values (*12*). They result primarily from the tendency of the sea surface to remain near equilibrium with atmospheric CO_2 at different temperatures. This conclusion is demonstrated by the curve shown in Fig. 1b, which was calculated

0036-8075/79/0615-1203$00.50/0

by assuming equilibration of a single average surface seawater with an atmospheric pCO_2 of 325 μatm over the range of sea surface temperatures (*13*).

The small errors associated with B_{hom} are surprising in view of the fact that pCO_2 values calculated by using the various sets of dissociation constants typically vary by 10 to 20 percent. The homogeneous buffer factor is partially protected from these errors because simultaneous errors in the partial derivative $(\partial pCO_2/\partial TCO_2)_{TA}$ and in the normalizing ratio TCO_2/pCO_2 tend to cancel each other. Thus, B_{hom} for a given seawater sample may be better known than its pCO_2.

Table 1. Net global anthropogenic CO_2 transfers to the ocean mixed layer calculated by using different sets of equilibrium constants: (A) Lyman (*4*) and Weiss (*16*), (B) Mehrbach *et al.* (*6*) and Weiss (*16*), (C) Hansson (*7*) and Weiss (*16*), (D) Buch (*3*) and Weiss (*16*), (E) Edmond and Geiskes (*5*) and Weiss (*16*), (F) Edmond and Gieskes (*5*) and Li and Tsui (*15*). A uniform mixed-layer depth of 100 m was assumed. Numbers in parentheses are percentage differences relative to row A: percentage difference = 100(x − row A value)/(row A value). Values are Σ(area × TCO_2 increase × density × mixed-layer depth) at the atmospheric CO_2 partial pressures shown.

Constant	Carbon ($\times 10^{15}$ moles) at pCO_2 of				
	325 μatm	400 μatm	600 μatm	1200 μatm	1800 μatm
A	0	1.492	4.170	8.075	10.119
B	0	1.485 (−0.5)	4.149 (−0.5)	8.029 (−0.6)	10.061 (−0.6)
C	0	1.487 (−0.3)	4.156 (−0.3)	8.045 (−0.4)	10.080 (−0.4)
D	0	1.537 (3.0)	4.313 (3.4)	8.386 (3.8)	10.515 (3.9)
E	0	1.484 (−0.5)	4.139 (−0.7)	7.991 (−1.0)	10.005 (−1.1)
F	0	1.475 (−1.3)	4.111 (−1.4)	7.936 (−1.7)	9.942 (−1.7)

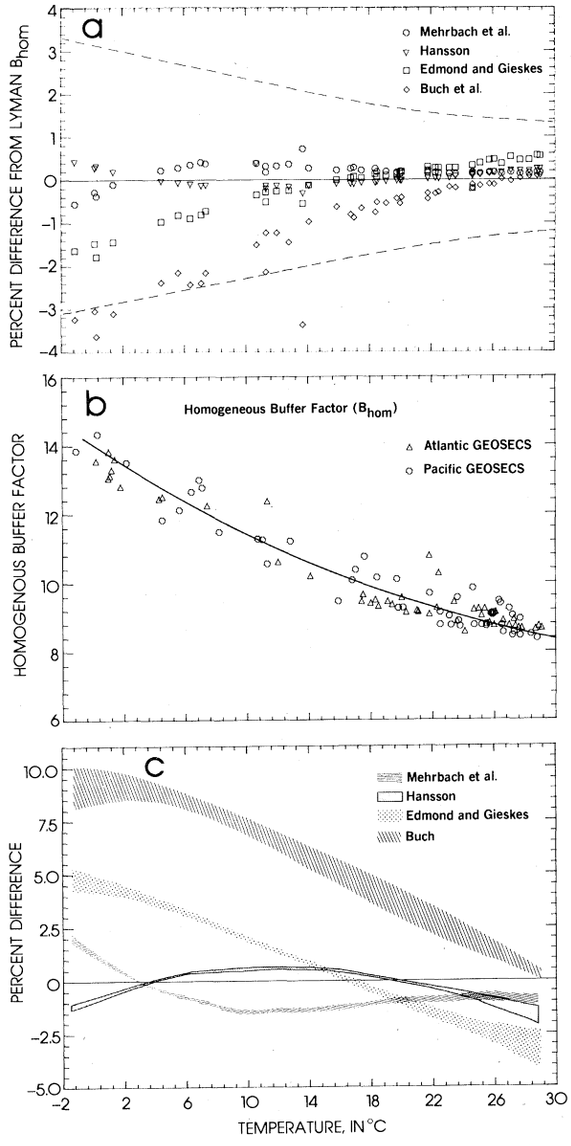

Fig. 1. (a) Percentage differences in B_{hom} values calculated from GEOSECS TCO_2 and TA data (*9*) for 40 representative stations, using the published sets of apparent dissociation constants (*3*–*8*). The curves show percentage differences in B_{hom} values generated by ± 0.5 percent differences in the TCO_2 or TA data when B_{hom} is calculated with Lyman's constants (*4*). (b) Values of B_{hom} calculated from GEOSECS TCO_2 and TA data (*9*). (c) Percentage differences in increases of ocean surface TCO_2 calculated by using the various sets of dissociation constants. The TCO_2 increase is the difference between the TCO_2 in equilibrium with a pCO_2 of 325 μatm and that in equilibrium with a higher pCO_2. Each shaded band shows the full range of relative differences over the pCO_2 range 400 to 1800 μatm. Percentage differences for (a) and (c) were calculated relative to values determined with Lyman's constants: percentage difference = 100 (x − Lyman)/(Lyman), where x is the value being compared.

Global CO_2 models are subject to the combined effects of errors in both B_{hom} and pCO_2. To assess the significance of these errors, it is very useful to note that air-sea gas exchange appears to be rapid enough to ensure that ocean mixed layer TCO_2 levels will remain very close to equilibrium with respect to future atmospheric CO_2 levels. This relationship is apparent in all current global CO_2 models (*14*). Thus, the transfer of CO_2 from the atmosphere into the ocean surface can be closely approximated by increases in ocean surface TCO_2 values in equilibrium with rising pCO_2 values.

Figure 1c compares the increases in ocean surface TCO_2 values calculated with the published sets of equilibrium constants. Initial TCO_2 values for 97 representative GEOSECS stations in the Atlantic and Pacific oceans were calculated by assuming equilibrium with an initial pCO_2 of 325 μatm at the measured temperature, salinity, and TA for each station. The TCO_2 increases relative to these initial values were then calculated at pCO_2's ranging from 400 to 1800 μatm. If the constants of Buch (*3*) and Edmond and Gieskes (*5*) are rejected, the maximum difference is less than 3 percent at all temperatures. Small additional differences (< 1 percent) are generated by using the different CO_2 solubilities of Li and Tsui (*15*) and Weiss (*16*).

To estimate the net future global transfer of anthropogenic CO_2 from the atmosphere into the ocean mixed layer, the TCO_2 increases used to derive Fig. 1c were averaged over each of seven latitude zones. Ocean surface areas corresponding to these zones (*17*) were then used to calculate the area-adjusted global CO_2 fluxes into the mixed layer for each published set of constants. Table 1 shows that without the constants of Buch (*3*) and Edmond and Gieskes (*5*), the calculated fluxes agree within 1 percent. A 1 percent error in the present estimated rate of increase of TCO_2 in the ocean surface is equivalent to an uncertainty of about 4×10^{11} moles of carbon per year (*18*). In comparison, the flux of fossil fuel CO_2 into the atmosphere is approximately 5×10^{14} moles of carbon per year (*19*). Analytical uncertainties in the net flux of carbon into the global ocean mixed layer therefore constitute an insignificant fraction (< 1 percent) of the total anthropogenic CO_2 budget.

To assess the transfer of anthropogenic CO_2 to the oceans as a whole, it is necessary to consider the extent to which ocean surface increases in TCO_2 will affect the exchange of carbon with deeper waters. In both the advective and diffusive approaches to modeling vertical ocean mixing, the flux of anthropogenic CO_2 into the deep ocean is directly proportional to the amount of anthropogenic CO_2 in the mixed layer (*20, 21*). Thus, a 1 percent error in the mixed layer TCO_2 increase will generate a 1 percent error in the deep ocean TCO_2 increase. In comparison, advective and diffusive ocean mixing parameters are presently associated with uncertainties of at least 50 percent (*22*). These uncertainties are compounded by the unknown but nonnegligible involvement of horizontal transport processes. Present uncertainties in the nature of ocean mixing therefore completely overshadow uncertainties that might be generated by errors in the ocean surface TCO_2 increase.

Uncertainties in terrestrial carbon fluxes also contribute significantly to the monumental difficulty of modeling the global CO_2 system. For example, the range of estimates for the flux of CO_2 into the atmosphere from deforestation (*23*) exceeds the magnitude of the present annual flux from combustion of fossil fuels and is far greater than the range of errors in the CO_2 balance that might be attributed to homogeneous buffer factor measurements and calculations.

The global CO_2 problem requires an urgent effort to fill fundamental gaps in our knowledge of the global carbon system. In attempting to establish research priorities that will provide the quickest answers to the most important questions, the scientific community must carefully ascertain what we know as well as what we do not know. The homogeneous equilibrium behavior of dissolved inorganic carbon in surface seawater seems to be one of the best-known aspects of the present and future global CO_2 budget.

E. T. SUNDQUIST
L. N. PLUMMER
U.S. Geological Survey, Reston, Virginia 22092
T. M. L. WIGLEY
Climatic Research Unit, University of East Anglia, Norwich, NR4 7TJ England

References and Notes

1. *A Comprehensive Plan for Carbon Dioxide Effects Research and Assessment*, part I, *The Global Carbon Cycle and Climatic Effects of Increasing Carbon Dioxide* (Office of Carbon Dioxide Effects Research and Assessment, Department of Energy, Washington, D.C., 1978), p. 27.
2. See, for example, R. Revelle and H. E. Suess, *Tellus* **9**, 18 (1957); B. Bolin and E. Eriksson, in *The Atmosphere and the Sea in Motion*, B. Bolin, Ed. (Rockefeller Univ. Press, New York, 1959), p. 130.
3. K. Buch, *Hayforsk. Inst. Skr. 151* (1951).
4. J. Lyman, thesis, University of California, Los Angeles (1956).
5. J. M. Edmond and J. M. T. M. Gieskes, *Geochim. Cosmochim. Acta* **34**, 1261 (1970).
6. C. Mehrbach, C. H. Culberson, J. E. Hawley, R. M. Pytkowicz, *Limnol. Oceanogr.* **18**, 897 (1973).
7. I. Hansson, *Deep-Sea Res.* **20**, 461 (1973).
8. The different sets of dissociation constants were calculated by using the equations given and cited by Takahashi *et al.* (*10*, appendix).
9. We used the titration TCO_2 and TA data from the GEOSECS leg reports, corrected according to the recommendations of Takahashi *et al.* (*10*) and Broecker and Takahashi (*11*), to calculate the necessary concentrations as functions of the GEOSECS salinities and temperatures.
10. T. Takahashi, P. Kaiteris, W. S. Broecker, A. E. Bainbridge, *Earth Planet. Sci. Lett.* **32**, 458 (1976).
11. W. S. Broecker and T. Takahashi, *Deep-Sea Res.* **25**, 65 (1978).
12. Latitudinal variations of the buffer factor were also noted by Keeling (*20*) and by R. M. Pytkowica and L. F. Small [in *The Fate of Fossil Fuel CO_2 in the Oceans*, N. R. Anderson and A. Malahoff, Eds. (Plenum, New York, 1977), p. 7].
13. The global atmospheric pCO_2 was very close to 325 μatm during the period 1972 to 1974, when the GEOSECS data were collected. The average salinity and TA of surface seawater, calculated from the GEOSECS data by a method that weighted latitudinal zones according to their surface areas (*17*), were 35.05 per mil and 2330 μEq/kg.
14. For example, see (*20, 21*). Although ocean surface pCO_2 values are seldom in equilibrium with the atmosphere (W. S. Broecker, T. Takahashi, H. J. Simpson, T. H. Peng, *Science*, in press), the disequilibrium does not significantly affect ocean surface TCO_2 or B_{hom} values.
15. Y.-H. Li and T.-F. Tsui, *J. Geophys. Res.* **76**, 4213 (1971). Fugacity corrections were applied according to the recommendations of P. Kaiteris and T. Takahashi [interim report on grant IDO72-06419 submitted to the National Science Foundation (1975)].
16. R. F. Weiss, *Mar. Chem.* **2**, 203 (1974).
17. H. U. Sverdrup, M. W. Johnson, R. H. Fleming, *The Oceans* (Prentice-Hall, Englewood Cliffs, N.J., 1942), p. 13.
18. This figure is calculated from the approximate rate of increase of TCO_2 (1 μmole/kg-year) implied by sea surface equilibrium with the atmosphere at the measured rate of atmospheric increase.
19. C. F. Baes, H. E. Goeller, J. S. Olson, R. M. Rotty, *The Global Carbon Dioxide Problem* (ORNL-5194, Oak Ridge National Laboratory, Oak Ridge, Tenn., 1976).
20. C. D. Keeling, in *Chemistry of the Lower Atmosphere*, S. I. Rasool, Ed. (Plenum, New York, 1973), p. 251.
21. U. Siegenthaler and H. Oeschger, *Science* **199**, 388 (1978).
22. For example, H. Stommel and A. B. Arons, *Deep-Sea Res.* **6**, 217 (1960); H. H. Kuo and G. Veronis, *ibid.* **17**, 29 (1970); M. Stuiver, unpublished manuscript.
23. G. M. Woodwell, R. H. Whittaker, W. A. Reiners, G. E. Likens, C. C. Delwiche, D. B. Botkin, *Science* **199**, 141 (1978).
24. Further details of calculations are available from E.T.S. We thank T. Takahashi, W. Broecker, D. Spencer, J. Edmond, R. Baier, and A. Bainbridge for access to the GEOSECS leg reports. M. Stuiver kindly provided unpublished eddy diffusion coefficient estimates. Discussions with T. Takahashi were particularly helpful. Some of this work was made possible by support from NSF grant OCE75-21210 to R. Siever while E.T.S. was his graduate student.

15 December 1978; revised 5 March 1979

Phospholipid Methylation Unmasks Cryptic β-Adrenergic Receptors in Rat Reticulocytes

Abstract. *The effect of phospholipid methylation on the number of β-adrenergic receptor binding sites was examined in rat reticulocyte membranes. Stimulation of phosphatidylcholine synthesis by the introduction of the methyl donor* S-*adenosyl-*L-*methionine into reticulocyte ghosts increased the number of β-adrenergic receptor binding sites. The appearance of β-adrenergic binding sites was dependent on the formation of phosphatidylcholine by the enzyme that converts phosphatidyl-*N-*monomethylethanolamine to phosphatidylcholine, but not on the synthesis of phosphatidyl-*N-*monomethylethanolamine from phosphatidylethanolamine. Both the synthesis of phosphatidylcholine and the unmasking of cryptic receptors were time and temperature dependent and did not occur in the presence of the methyl transferase inhibitor,* S-*adenosyl-*L-*homocysteine.*

Two membrane-bound enzymes are present in adrenal medulla, erythrocytes, and reticulocytes that synthesize phosphatidylcholine by successive *N*-terminal methylations of phosphatidylethanolamine (*1*). Both the enzymes and their products are asymmetrically distributed in the membrane. Methyltransferase I is located on the cytoplasmic side of the membrane and converts phosphatidylethanolamine to phosphatidyl-*N*-monomethylethanolamine. This enzyme has a high affinity (Michaelis constant, K_m, = 1 μM) for the methyl donor, *S*-adenosyl-L-methionine, and requires Mg^{2+}. Methyltransferase II, located on the external side of the membrane, adds two methyl groups to phosphatidyl-*N*-monomethylethanolamine to form phosphatidylcholine. This enzyme has a low affinity (K_m = 100 μM) for *S*-adenosyl-L-methionine and does not require Mg^{2+}. By these enzymatic reactions phosphatidylethanolamine, on the cytoplasmic side of the reticulocyte membrane, is methylated to phosphatidylcholine and rapidly translocated to the external side of the membrane (*1*).

Rat reticulocyte membranes contain relatively large numbers of β-adrenergic receptors (*2*). Stimulation of β-adrenergic receptors increases the activity of both methylating enzymes, particularly methyltransferase II (*3*). The elevation of phospholipid methylation depends on

0036-8075/79/0615-1205$00.50/0